

Journal of Applied Pharmaceutical Research Volume 13 Issue 4, Year of Publication 2025, Page 298 – 312 DOI: https://doi.org/10.69857/joapr.v13i4.1167



## **Research Article**

## JOURNAL OF APPLIED PHARMACEUTICAL RESEARCH | JOAPR

www.japtronline.com ISSN: 2348 – 0335

### FORMULATION, DESIGNING AND EVALUATION OF GASTRO-RETENTIVE FLOATING MICROSPHERES USING SILYMARIN, CURCUMIN AND PIPERINE FOR HEPATOPROTECTION

Misbah Sultana Abdul Kausar Badewale<sup>1, 2\*</sup>, Varsha Siddheswar Tegeli<sup>2</sup>

#### **Article Information**

Received: 2<sup>nd</sup> May 2025 Revised: 28<sup>th</sup> June 2025 Accepted: 18<sup>th</sup> July 2025 Published: 31<sup>st</sup> August 2025

#### Keywords

Gastro-retentive, Microspheres, Curcumin, Silymarin, Piperine, Hepatoprotection, Ethyl cellulose.

#### ABSTRACT

Background: Curcumin, Silymarin, and Piperine are natural phytoconstituents with proven hepatoprotective effects; however, their therapeutic efficacy is limited by poor water solubility and low oral bioavailability. A gastro-retentive floating drug delivery system offers a strategic approach to enhance gastric residence time and improve absorption in the upper gastrointestinal tract. Methodology: Floating microspheres were developed using the solvent evaporation technique with Ethyl Cellulose and Eudragit RS 100 as polymers. A series of trial formulations was statistically optimized using Design Expert® software. The microspheres were evaluated for particle size, buoyancy, entrapment efficiency, drug release profile, and stability. Results and Discussion: The optimized formulation (Batch F3) demonstrated high encapsulation efficiency (>98%) and sustained buoyancy of 95.94% over 8-hour. At the end of 12 hours, cumulative drug release was 66.24% for Curcumin, 68.21% for Silymarin, and 72.82% for Piperine. Drug release followed zero-order kinetics, with the best model fit (R² = 0.9938) observed for Piperine. SEM images confirmed the presence of spherical and uniform microspheres. The formulation remained stable for 90 days under ICH Q1A(R2) conditions. Conclusion: The developed microspheres offer a promising gastroretentive system for controlled delivery of hepatoprotective agents, potentially improving therapeutic outcomes for liver-related disorders.

#### INTRODUCTION

Oral administration is the most commonly utilized and preferred drug delivery method, primarily due to its ease of use, high patient adherence, and economic viability. Nevertheless, this route presents significant challenges stemming from the complex physiology & dynamic transit characteristics of the GIT, often leading to irregular drug absorption. Such inconsistencies may hinder optimal drug bioavailability &

therapeutic efficacy, particularly in the case of compounds with a narrow absorption window or limited solubility in alkaline conditions. To address these shortcomings, gastroretentive drug delivery systems (GRDDS) have been developed to provide controlled drug release within the stomach [1]. Various strategies have been adopted to extend gastric residence time (GRT), such as high-density dosage forms, expandable systems, mucoadhesive approaches & floating drug delivery systems

#### \*For Correspondence: misbahp1@yahoo.com @2025 The authors

This is an Open Access article distributed under the terms of the Creative Commons Attribution (CC BY NC), which permits unrestricted use, distribution, and reproduction in any medium, as long as the original authors and source are cited. No permission is required from the authors or the publishers. (https://creativecommons.org/licenses/by-nc/4.0/)

<sup>&</sup>lt;sup>1</sup>Punyashlok Ahilyadevi Holkar Solapur University, Solapur-Pune National Highway, Kegaon, Solapur 413255, Maharashtra, India. <sup>2</sup>D.S.T.S. Mandal's College of Pharmacy, Solapur 413255, Maharashtra, India.

(FDDS). These technologies aim to improve drug bioavailability, minimize degradation and waste, and facilitate localized drug action within the stomach and proximal small intestine [2-3].

Piperine, a known bioenhancer, inhibits hepatic and intestinal glucuronidation, enhancing the absorption of both Silymarin and Curcumin. Studies have demonstrated that the combination of these agents exhibits synergistic hepatoprotective effects against alcohol-induced and chemically induced liver damage. Within the FDDS category, non-effervescent floating microspheres are particularly noteworthy due to their ability to maintain sustained buoyancy without altering gastric emptying patterns.

These microspheres, typically formed from polymers like ethyl cellulose, hydroxypropyl methylcellulose (HPMC), chitosan, and polycarbonate, possess a lower bulk density than gastric fluids, allowing them to float and provide prolonged drug release. This sustained delivery minimizes plasma level fluctuations, reduces dosing frequency, and mitigates risks such as dose dumping [4-5]. Their preparation is commonly carried out using emulsion solvent evaporation and solvent diffusion techniques, with formulation variables such as polymer type, plasticizer content, and solvent selection influencing both floatation and release profiles [6-7]. Liver disorders are a significant global health concern, contributing substantially to disease burden and death rates. In fact, liver cirrhosis is identified as the 12th leading cause of death in the United States by the National Institute on Alcohol Abuse and Alcoholism [8].

This condition is further aggravated by factors like obesity, sedentary behavior, excessive alcohol intake, and misuse of medications [9-10]. Therefore, liver protection is a key objective in therapeutic research. Natural compounds such as Silymarin (derived from Silybum marianum) [11-12], Curcumin (from Curcuma longa) [13], and Piperine (from Piper nigrum) have demonstrated robust liver-protective, antioxidant, and anti-inflammatory effects, and are frequently used in herbal remedies targeting liver health.

Despite these benefits, their clinical application is hampered by poor water solubility, limited absorption, and rapid systemic clearance, resulting in low bioavailability. However, the hepatoprotective roles of these compounds have been extensively investigated both individually and in combination.

There is a notable gap in research focused on a gastroretentive multiparticulate delivery system that can co-administer these actives through floating microsphere technology.

This study aims to formulate and assess a gastroretentive floating microsphere system containing Curcumin [14], Silymarin [15-16], and Piperine [17], utilizing ethyl cellulose and Eudragit RS 100 via the solvent evaporation method. The objective is to achieve prolonged gastric retention, controlled drug release, and enhanced liver-protective efficacy through optimized encapsulation and delivery mechanisms.

#### MATERIALS AND METHODS Chemicals and Reagents

The samples of Curcumin, Silymarin, and Piperine were provided by Aadhaar Life Sciences Pvt. Ltd. Acetonitrile was purchased from Qualigens, Mumbai. Ethyl Cellulose, Eudragit RS 100, and HPMC were purchased from Banglor File Chemicals. Carbopol 974P was made available by Lubrizol, and Span 80 was purchased from Croda, India. Perchloric acid was purchased from Merck Life Sciences Pvt. Ltd., Mumbai. Weighing was conducted utilizing calibrated NABL scales. Samples were prepared in Type A glassware and measured using the analytical balance.

## **METHODOLOGY Pre-formulation studies**

#### Solubility Analysis

The solubility profiles of Curcumin, Silymarin, and Piperine were evaluated in various solvents to determine suitable carriers and solvents for formulation. The solubility was determined by the shake flask method at room temperature. Samples were qualitatively observed and further quantified spectrophotometrically, where applicable.

#### **Melting Point Determination**

The melting point of all three active compounds was determined using the capillary tube method to confirm purity and identity.

#### Drug-drug and Drug-Excipient compatibility study

Physical mixtures of each Drug with polymers, such as ethyl cellulose, HPMC, Carbopol 974P, and Eudragit RS 100, were prepared by mixing in a 1:1 ratio and subjected to FTIR analysis using the KBr pellet method.

# Formulation & optimization of Gastro-retentive Floating microspheres

In beaker-A, 10 mL of DCM and 10 mL of Methanol were taken. To it, the polymer and drug were dissolved and mixed for 10 minutes. In beaker B, 100 mL of water containing 0.01% Span 80 was added and mixed at 500 rpm using an overhead mixer at 30°C. The content of beaker A was then added in a thin stream with continuous mixing. The mixing was carried out for 2 hours until all the organic solvent was evaporated. The above mixture was filtered, and the residue was washed using 50 ml of water to

remove any residual organic solvent. The residue collected on the filter paper was dried in a hot air oven at 40°C overnight and then collected for further evaluation, as shown in Table 1. Span 80 (0.01%) was used as a surfactant to stabilize the emulsion droplets by reducing interfacial tension. The low concentration was chosen to prevent foaming and ensure the formation of spherical particles. An overhead stirrer equipped with a Teflon blade (IKA RW20) was used at 500 rpm. Droplet size was indirectly controlled by adjusting stirring speed and surfactant concentration.

**Table 1: Composition of Floating Microsphere Batches (F1–F9)** 

S. No.	Ingredients (mg)	F1	F2	F3	F4	F5	F6	F7	F8	F9
1	Curcumin	100	100	100	100	100	100	100	100	100
2	Silymarin	100	100	100	100	100	100	100	100	100
3	Piperine	100	100	100	100	100	100	100	100	100
4	Ethyl Cellulose	450	150	450	300	300	450	150	300	150
5	Eudragit RS 100	150	300	450	450	300	300	150	150	450
6	0.01% Span 80 ml	100	100	100	100	100	100	100	100	100

### Evaluation of gastro-retentive floating microspheres Percentage Yield

The percentage yield of microspheres was calculated by comparing the weight of the dried microspheres to the total initial weight of the drug and polymer used during their formulation [18]. The following formula was applied to determine the % yield.

$$\% Yield = \frac{Practical \ yield \ (mg)}{Theoretical \ yield \ (mg)} \times 100$$

#### **Drug Content**

After precisely weighing 10 mg of the standard in a 10-ml volumetric flask, 5 mL of diluent was added, and the solution was dissolved, bringing the volume up to 10 mL. 1 mL was taken and then further diluted to 10 mL.

$$\% \ drug \ content = \frac{Sample \ area}{standard \ area} \\ \times \frac{standard \ concentration}{sample \ concentration} \\ \times potency \ of \ standard$$

#### Entrapment efficiency

An accurately weighed 100 mg sample of microspheres was finely ground using a mortar, followed by the addition of 100 mL of diluent. This mixture was subjected to sonication to facilitate complete dissolution. From this homogenized suspension, a 1 ml portion was withdrawn and subsequently diluted to a final volume of 10 ml. The resulting solution was

filtered and analyzed using a UV spectrophotometer at 215 nm to quantify the free drug present [19-20]. The method was validated for linearity ( $r^2 > 0.998$ ), precision (RSD < 2%), and accuracy (recovery 98–102%). The entrapment efficiency was then determined using the following equation:

$$\% \ Entrapment \ efficiency \\ = \frac{calculated \ drug \ concentration}{theoretical \ drug \ content} \times 100$$

#### In-vitro Buoyancy

The floating behavior of the microspheres was evaluated using a USP Type II dissolution apparatus. A 100 ml volume of 0.1N hydrochloric acid, serving as the simulated gastric fluid, was used as the dissolution medium. The medium was stirred with a paddle rotating at 100 rpm. 100 mg of microspheres were selected as a standard sample for buoyancy studies. Floating lag time was observed to be <10 seconds for all formulations. Following 8 hours of continuous agitation, the microspheres remaining afloat and those that had settled at the bottom were collected separately [21]. After drying, each portion was weighed, and the buoyancy percentage was calculated using the following formula:

$$\%$$
 Buoyancy =  $\frac{Qf}{(Qf + Qs)} \times 100$ 

Where, QF = Weight of the floating microspheres, Qs = Weight of the settled microspheres.

#### Particle size

The particle size was measured using a Horiba SZ-100 (Horiba Scientific) at a temperature of 25 °C. A disposable sizing cuvette was utilized, maintaining constant values for refractive index, viscosity, and dielectric constant.

Since DLS is not suitable for microspheres larger than 1  $\mu$ m, optical microscopy using ImageJ software was employed to analyze the size and distribution of the microspheres, the nanocarrier samples were diluted in deionized water to an appropriate concentration and subsequently analyzed using the instrument.

#### In vitro drug release studies

The in vitro drug release of the formulation was conducted using a USP Type II dissolution apparatus, operated at 100 rpm and maintained at 37°C in 0.1 N hydrochloric acid, over a 12-hour period. At predetermined intervals, 5 mL samples were withdrawn and immediately replaced with an equal volume of fresh dissolution medium to preserve sink conditions. The collected samples were filtered through a 0.45  $\mu m$  membrane filter and analyzed spectrophotometrically at 215 nm using a UV-visible spectrophotometer.

#### Release kinetics

The in vitro drug release data from the floating microspheres were analyzed using various kinetic models, including zero-order, First-order, Higuchi, and Korsmeyer-Peppas models, to understand the release mechanism and rate of drug diffusion [22].

#### Surface morphology by SEM

The morphology and shape of the floating microspheres were examined through scanning electron microscopy. Various formulations were randomly selected for imaging, and micrographs were captured at appropriate magnifications [23].

#### Stability study of Microspheres

Stability testing was conducted in accordance with the guidelines established by the ICH. The optimized floating microsphere formulation (F3) was stored at 40 °C  $\pm$  2 °C and 75%  $\pm$  5% relative humidity to assess its stability. Assessments of drug content and in vitro drug release were conducted on the initial day (0th) and after 90 days of storage. The study was conducted in accordance with the ICH Q1A(R2) guidelines.

# RESULTS AND DISCUSSION Pre-formulation studies Solubility

**Table 2: Solubility of drugs** 

Drug	Solubility
	Curcumin was soluble in Dichloromethane and
Curcumin	acetone; sparingly soluble in Acetonitrile,
	methanol, ethanol, isopropyl alcohol & water.
Cilymanin	Silymarin was soluble in methanol, ethanol,
Silymarin	and DMSO. It was slightly soluble in water.
	Piperine was soluble in Dichloromethane,
Piperine	acetone, methanol, and ethanol. It was slightly
	soluble in acetonitrile and insoluble in water.

#### Melting point

The melting points for Curcumin, Silymarin, and Piperine were found to be:

**Table 3: Melting point of drugs** 

Sr. No.	Compound	Melting point (°C)
1	Curcumin	182.5
2	Silymarin	159.0
3	Piperine	128.5

#### FTIR of drugs

The FTIR spectra were recorded to evaluate possible interactions between the active pharmaceutical ingredients (Curcumin, Silymarin, and Piperine) and the excipients used in the microsphere formulation. Curcumin showed characteristic peaks at  $\sim\!3500~{\rm cm^{-1}}$  (O–H stretching) and  $\sim\!1600~{\rm cm^{-1}}$  (aromatic C=C stretching). Silymarin exhibited O–H stretching between 3400–3200 cm<sup>-1</sup> and aromatic ring vibrations near 1600 cm<sup>-1</sup>.

Piperine presented notable peaks at ~2920 cm<sup>-1</sup> (C–H stretching), ~1640 cm<sup>-1</sup> (C=O stretching), and aromatic C=C stretching around 1600 cm<sup>-1</sup>. The drug-excipient mixture displayed all major peaks corresponding to individual drugs without significant shifting or loss, confirming the absence of chemical interaction and indicating compatibility between drugs and excipients.

#### Formulation and optimization of Floating Microspheres

Based on Pre-formulation data, all three APIs were combined with the Excipient to form microspheres. The microspheres were formulated using the Solvent-Evaporation method. Initially, nine prototypes were developed with different concentrations of

excipients. DCM and methanol were selected due to their volatility and solubilizing capacity for both drug and polymer.

Residual solvents were removed by evaporation over 2 hours and confirmed using weight constancy and absence of odor.

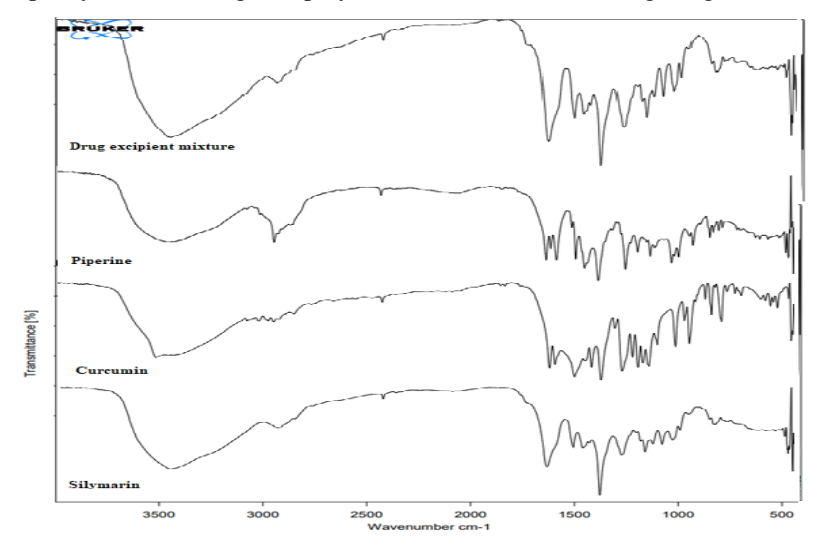


Figure 1: FTIR Spectra of Curcumin, Silymarin, Piperine, and Drug-Excipient Mixture

#### **Evaluation of gastro-retentive floating microspheres**

**Percentage Yield:** The percentage yield was calculated for all nine prototypes, and the results for % yield are given below:

Table 4: Percentage yield of prototypes of microspheres

SN	Batch	Practical yield	Theoretical yield	%
514	Daten	(mg)	(mg)	Yield
1	F1	861.0	900	95.67
2	F2	695.6	750	92.75
3	F3	1178.9	1200	98.62
4	F4	1023.0	1050	97.43
5	F5	860.3	900	95.59
6	F6	1010.2	1050	96.21
7	F7	591.7	600	98.24
8	F8	699.4	750	93.25
9	F9	848.2	900	94.24

The Formulation F3 shows the highest % yield of 98.62%.

**Drug Content:** The drug content percentage was determined using the HPLC method, and the outcomes are presented in Table 5. HPLC was employed for quantification to resolve the overlapping absorption peaks of Curcumin, Silymarin, and Piperine, which share an absorbance maximum around 215 nm.

**Percentage Encapsulation Efficiency:** Table 6 presents the results of the encapsulation efficiency calculation

*In-vitro Buoyancy:* The percentage of buoyancy was evaluated, and it was found that all formulations remained afloat in the dissolution medium (0.1 N HCl) for a duration of 8 hours. The buoyancy % of the microspheres is presented in Table 7.

**Table 5: Percentage Drug content** 

Trial	% Drug content of Silymarin	% EE of Piperine	% EE of Curcumin
Trial 1	100.52	97.58	99.74
Trial 2	99.05	98.32	100.81
Trial 3	101.19	98.08	100.25
Trial 7	97.74	100.28	99.17
Trial 8	98.56	98.75	98.45
Trial 9	98.08	99.37	99.37

**Table 6: Percentage Encapsulation Efficiency** 

Trial	% EE of Silymarin	% EE of Piperine	% EE of Curcumin
Trial 1	95.73	96.42	95.17
Trial 2	97.20	97.83	96.28
Trial 3	98.24	99.57	98.09
Trial 7	96.20	98.03	96.94
Trial 8	97.97	98.45	98.45
Trial 9	99.07	99.07	99.37

Table 7: In-vitro Buoyancy of microspheres

Sr. No.	Batch	% Buoyancy
1	F1	79.26
2	F2	74.36
3	F3	95.94
4	F4	92.25
5	F5	81.45
6	F6	84.34
7	F7	63.21
8	F8	69.06
9	F9	89.22

Batch F3 yields the highest buoyancy of 95.94%.

**Particle size:** The results of Particle Size for microspheres were as mentioned in Table 8.

**Table 8: Particle Size of Gastro-retentive floating microspheres** 

Sr. No.	Batch	Particle Size (µm)
1	F1	183.4
2	F2	133.3
3	F3	208.7
4	F4	172.9

Sr. No.	Batch	Particle Size (µm)
5	F5	164.7
6	F6	191.3
7	F7	127.5
8	F8	152.5
9	F9	147.7

The findings indicated that the particle size of all formulations was reduced. Formulation F3 exhibited the lowest particle size, which was 127.5  $\mu$ m, as shown in Figure 2.

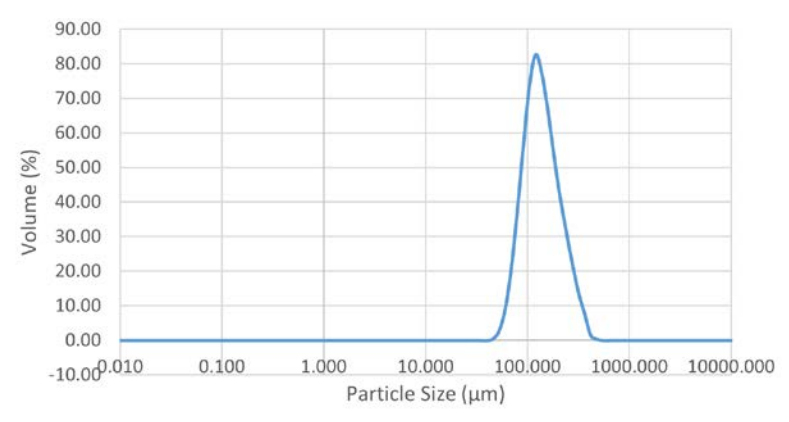


Figure 2: Particle Size distribution of F3

In vitro drug release studies: The results of drug release for Curcumin are shown in Table 9.

Table 9: In vitro drug release studies of Curcumin of Gastro-retentive Floating microspheres

	0				8 1					
Time (hr.)	F1	F2	F3	F4	F5	F6	F7	F8	F9	
0	0.00	0.00	0.00	0.00	0.00	0.00	0.00	0.00	0.00	
0.5	3.24	3.20	2.07	2.33	3.07	2.95	3.14	3.89	2.61	
1	6.47	6.33	4.80	5.19	6.19	5.96	7.21	6.39	5.47	
2	12.07	12.69	8.39	10.74	12.66	11.80	15.80	14.80	11.07	
3	18.36	18.75	14.19	16.55	18.34	17.86	18.38	17.25	16.98	
4	25.57	25.92	17.76	20.46	25.67	24.03	27.12	27.56	22.38	
6	37.55	36.77	27.26	30.42	36.55	35.78	38.18	37.73	34.03	
8	50.99	51.87	37.35	43.45	51.08	49.55	53.17	52.85	47.49	
12	75.43	73.18	66.24	67.11	72.57	71.66	76.20	75.76	68.16	

Batch F3 exhibited the slowest drug release, with an initial release of 2.07% at 1 hour & a cumulative release of 66.24% by 12 hr., indicating the gastro-retentive capacity of microspheres.

Figure 3 illustrates the graph depicting the relationship between cumulative drug release and time. The results of drug release for Silymarin are shown in Table 10.

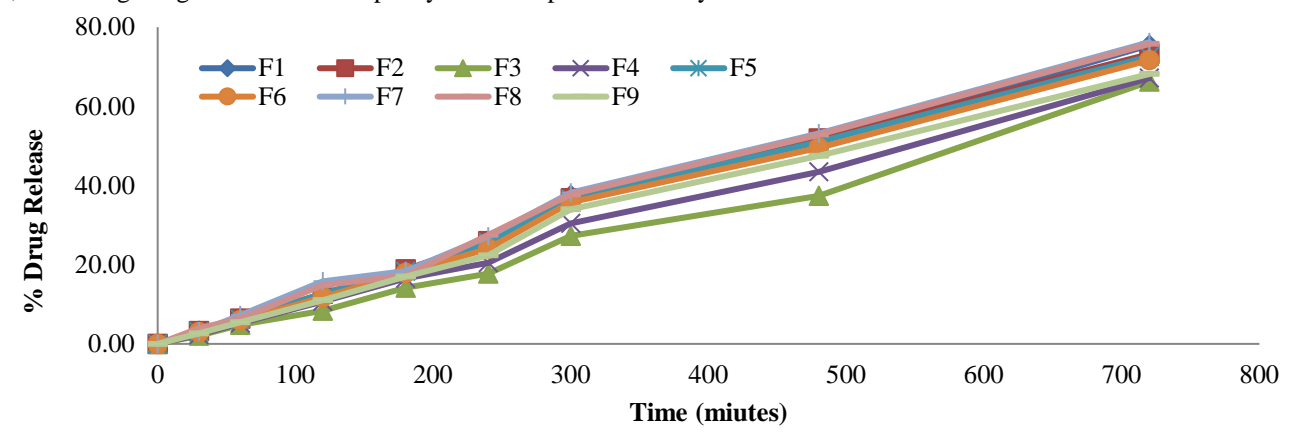


Figure 3: Graph showing % cumulative drug release vs time of Curcumin

Time (hr.)	<b>F</b> 1	F2	F3	F4	F5	F6	<b>F7</b>	F8	F9
0	0.00	0.00	0.00	0.00	0.00	0.00	0.00	0.00	0.00
0.5	3.20	3.33	2.55	3.09	3.24	3.01	3.63	3.43	3.27
1	6.28	6.74	5.82	6.12	6.38	6.09	7.06	6.76	6.58
2	13.56	14.03	11.79	12.99	13.55	12.38	14.56	14.19	13.79
3	18.68	19.55	17.38	18.28	18.90	18.27	20.79	20.18	18.98
4	27.13	28.62	23.20	27.12	27.65	25.36	30.19	29.14	27.62
6	37.15	39.42	34.79	36.67	37.15	36.14	41.37	40.22	39.04
8	54.67	56.49	46.86	54.14	54.79	51.37	61.42	58.24	55.93
12	75.62	78.12	68.21	73.70	74.07	72.17	80.54	79.24	77.41

Table 10: In vitro drug release studies of Silymarin of Gastro-retentive Floating microspheres

Batch F3 exhibited the slowest drug release, with an initial formulation percentage of 2.55% at 1 hour and 68.21% at 12 hours, indicating the gastro-retentive capability of Silymarin in

microspheres. Figure 4 illustrates the graph depicting the relationship between cumulative drug release and time. The drug release data for Piperine is presented in Table 11.

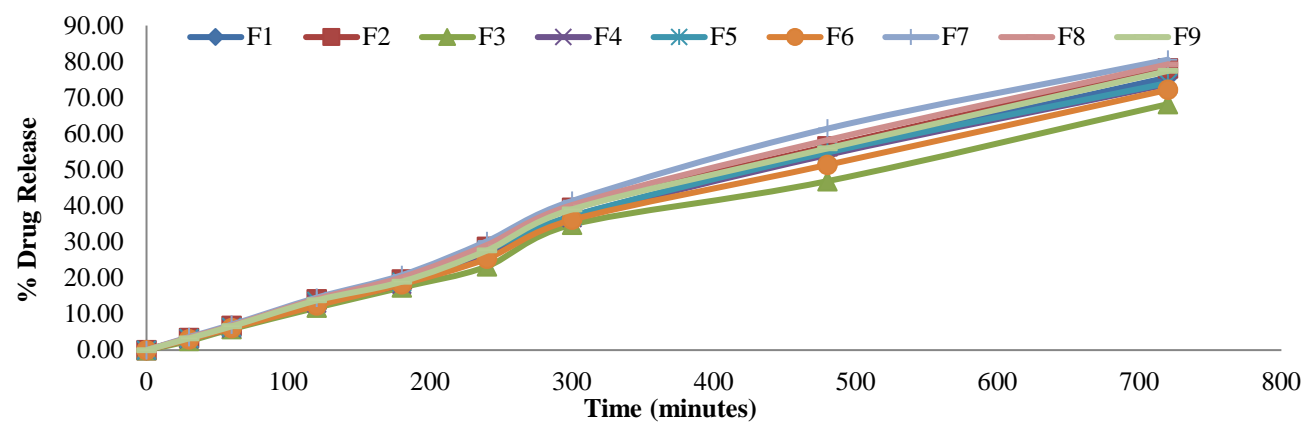


Figure 4: Graph showing % cumulative drug release vs time of Silymarin

Table 11: Evaluation of in vitro release profiles of Piperine from gastro-retentive floating microspheres

Time (hr.)	F1	F2	F3	F4	F5	<b>F6</b>	F7	F8	F9
0	0.00	0.00	0.00	0.00	0.00	0.00	0.00	0.00	0.00
0.5	3.85	3.65	3.27	3.32	3.57	3.46	3.93	3.75	3.37
1	7.06	6.88	6.40	6.45	6.75	6.64	7.86	7.55	6.51
2	14.17	13.80	12.58	12.89	13.54	13.32	16.27	15.58	13.05
3	20.74	20.21	18.46	18.69	19.43	19.25	22.20	21.86	18.81
4	28.50	27.47	25.77	26.03	27.07	26.61	31.09	30.16	26.30
6	41.27	40.13	37.29	38.09	39.21	38.74	45.22	42.88	38.39
8	55.32	54.55	51.64	52.10	54.27	53.37	62.76	61.36	52.20
12	82.33	80.09	72.82	73.91	78.71	77.46	85.90	83.62	75.35

Batch F3 exhibited the slowest drug release, with an initial release percentage of 3.27% at 1 hour and a total of 72.82% at 12 hours, indicating the gastro-retentive capability of piperine in microspheres. Figure 5 illustrates the graph depicting the relationship between cumulative drug release and time.

As the polymer concentration increased, a notable decrease in the total amount of drug released was observed. This effect can be attributed to the denser polymer network at higher concentrations, which results in a longer path for the drug molecules to diffuse through.

#### **Release Kinetics**

The in vitro drug release data were analyzed using various kinetic models, such as zero-order, first-order, Higuchi & Korsmeyer-Peppas, to determine which model best describes the drug release mechanism. The fitting profiles for Curcumin release are presented in Table 12.

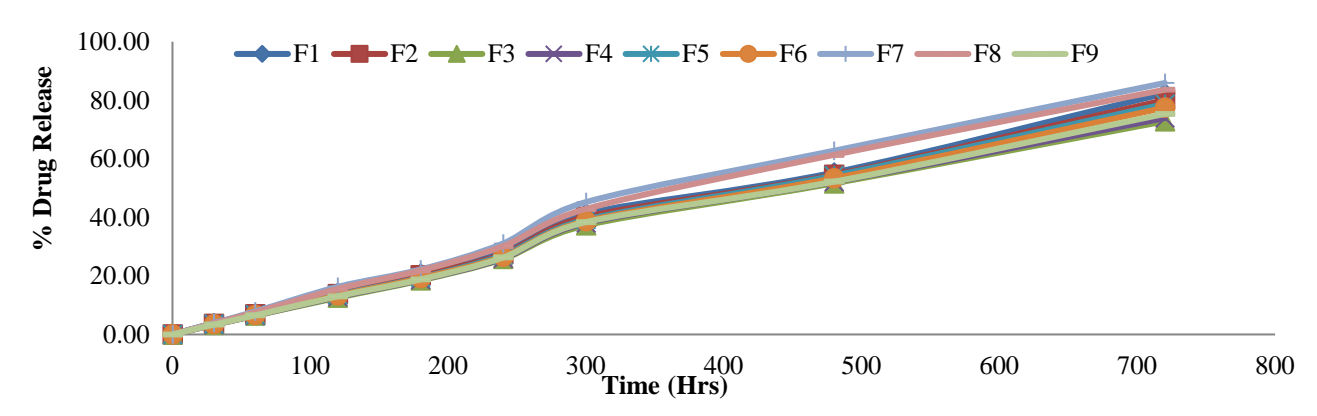


Figure 5: Piperine cumulative drug release vs. time graph

Table 12: Model fitting Curcumin release profile for formulations F1 to F9

Formulation	Zero Order (r <sup>2</sup> )	First order (r <sup>2</sup> )	Higuchi (r²)	KorsmeyerPeppas (r <sup>2</sup> )	
F1	0.9934	0.7353	0.9139	0.9264	
F2	0.9932	0.7277	0.9227	0.9273	
F3	0.9887	0.7898	0.8670	0.8756	
F4	0.9971	0.7560	0.9030	0.8962	
F5	0.9930	0.7291	0.9220	0.9236	
F6	0.9934	0.7388	0.9158	0.9180	
F7	0.9924	0.7093	0.9244	0.9323	
F8	0.9922	0.7214	0.9198	0.9391	
F9	0.9930	0.7463	0.9140	0.9052	

The Release kinetics data for Curcumin showed that the best-fit model for the F4 batch was Zero Order, with the highest R<sup>2</sup> value of 0.9971. Table 13 presents the model-fitting release profiles of Silymarin.

The Release kinetics data for Silymarin showed that the best-fit model for the F1 batch was Zero Order, with the highest R<sup>2</sup> value of 0.9936. Table 14 displayed Piperine's model-fitting release profiles.

Table 13: Silymarin's model-fitting release profile for formulations F1 to F9

Formulation	Zero Order (r <sup>2</sup> )	First order (r <sup>2</sup> )	Higuchi (r <sup>2</sup> )	KorsmeyerPeppas (r <sup>2</sup> )
<b>F1</b>	0.9936	0.7273	0.9217	0.9261
F2	0.9920	0.7195	0.9245	0.9309
F3	0.9920	0.7341	0.9194	0.9082
F4	0.9919	0.7290	0.9230	0.9222
F5	0.9914	0.7218	0.9265	0.9283
F6	0.9931	0.7321	0.9211	0.9210
<b>F7</b>	0.9880	0.7132	0.9265	0.9368
F8	0.9910	0.7179	0.9253	0.9323
F9	0.9919	0.7243	0.9214	0.9283

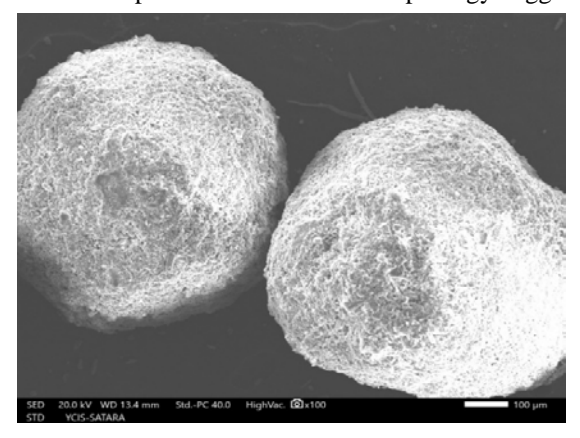
Table 14: Piperine's model-fitting release profile for formulations F1 to F9

Formulation	Zero Order (r <sup>2</sup> )	First order (r <sup>2</sup> )	Higuchi (r <sup>2</sup> )	Korsmeyer-Peppas (r <sup>2</sup> )
F1	0.9933	0.718	0.9186	0.9414
F2	0.9935	0.7215	0.9187	0.9376
F3	0.9917	0.7275	0.9222	0.9287
F4	0.9912	0.7257	0.9220	0.9298
F5	0.9938	0.7254	0.9179	0.9353
F6	0.9936	0.7264	0.9183	0.9330
F7	0.9888	0.7013	0.9275	0.9457
F8	0.9908	0.7065	0.9271	0.9423
F9	0.9922	0.7262	0.9201	0.9309

The Release kinetics data for Piperine showed that the best-fit model for the F5 batch was Zero Order, with the highest R<sup>2</sup> value of 0.9938.

#### Surface morphology by SEM

The surface morphology of the optimized formulation Batch F3 was examined using Scanning Electron Microscopy (SEM), as depicted in the micrographs. The SEM images were captured at magnifications of  $100\times$  and  $30\times$  to evaluate the surface characteristics and particle size distribution. At  $100\times$  magnification, the particles appear to be spherical with a relatively uniform shape & size. The surface of the microspheres shows a rough & porous texture, indicating the successful formation of the desired matrix structure. This porosity may enhance drug release by increasing surface area. At a lower magnification of  $30\times$ , a uniform distribution of microspheres is evident, without significant agglomeration. The size distribution seems consistent, supporting the reproducibility of the formulation process. The overall morphology suggests that the



particles are well-formed, with no visible cracks or deformities, implying good mechanical stability. These surface characteristics are critical for ensuring optimal drug encapsulation, sustained release, and predictable pharmacokinetics. The observed features confirm that Batch F3 has a desirable morphology for pharmaceutical application (Figure 6).

#### Stability study of Microspheres

The drug content and in vitro drug release of the samples were evaluated on the initial day and after 90 days. The comparative outcomes of the stability assessment are presented in Table 15. The formulation was found to be stable over a 90-day interval at  $40 \,^{\circ}\text{C} \pm 2 \,^{\circ}\text{C}$  and  $75\% \pm 5\%$  relative humidity. The formulation's in-vitro drug release & % drug content were marginally reduced.

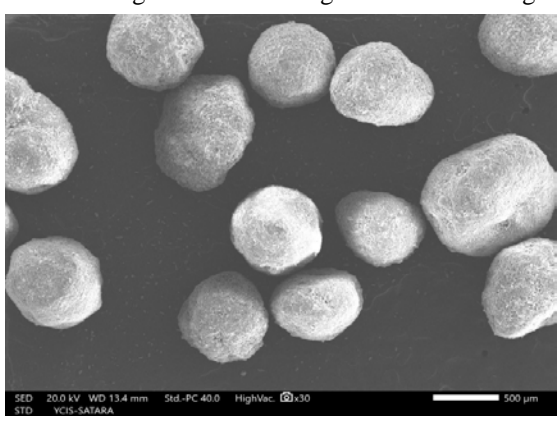


Figure 6: SEM Images of microspheres of formulation F3

Table 15: Results of Stability study of batch F3

Parameter _	Silymarin		Piperine		Curcumin	
	At 0th day	At 90th day after 12hr	At 0th day	At 90th day after 12hr	At 0th day	At 90 <sup>th</sup> day after 12hr
Drug Content(%)	98.33%	97.54%	97.25%	96.83%	98.18%	97.78%
In-vitro Drug Release	68.21%	68.09%	72.82%	72.46%	66.24%	65.94%

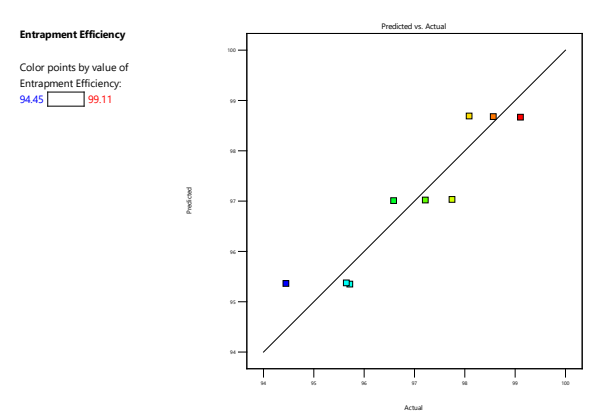
# Statistical optimization using Design Expert® software ANOVA spectra for Curcumin

#### **Response 1: Entrapment Efficiency**

Figure 7 presents a comparison between the observed and predicted values. The Adjusted R² value of 0.8342 closely aligns with the Predicted R² value of 0.7087, demonstrating a difference of less than 0.2, which is acceptable. It is recommended to perform confirmation experiments to validate all empirical models. The Entrapment Efficiency (EE) of curcumin surpasses 90% suggesting that both excipients contribute to its encapsulation. The contour plot (Figure 8)

reveals that as the concentration of ethyl cellulose increases, the entrapment efficiency of the microspheres improves.

Accordingly, a higher ethyl cellulose concentration leads to enhanced curcumin entrapment. Additionally, the 3D surface plot (Figure 9) shows that increasing the amount of Eudragit RS 100 causes a slight decline in entrapment efficiency, whereas raising the ethyl cellulose concentration results in an improvement in the curcumin entrapment within the microspheres.



Factor Coding: Actual

Entrapment Efficiency (%)

Design Points

X1 = A

X2 = B

Figure 7: Actual VS Predicted Plot- EE of Curcumin

**Figure 8: Contour Plot- EE of Curcumin** 

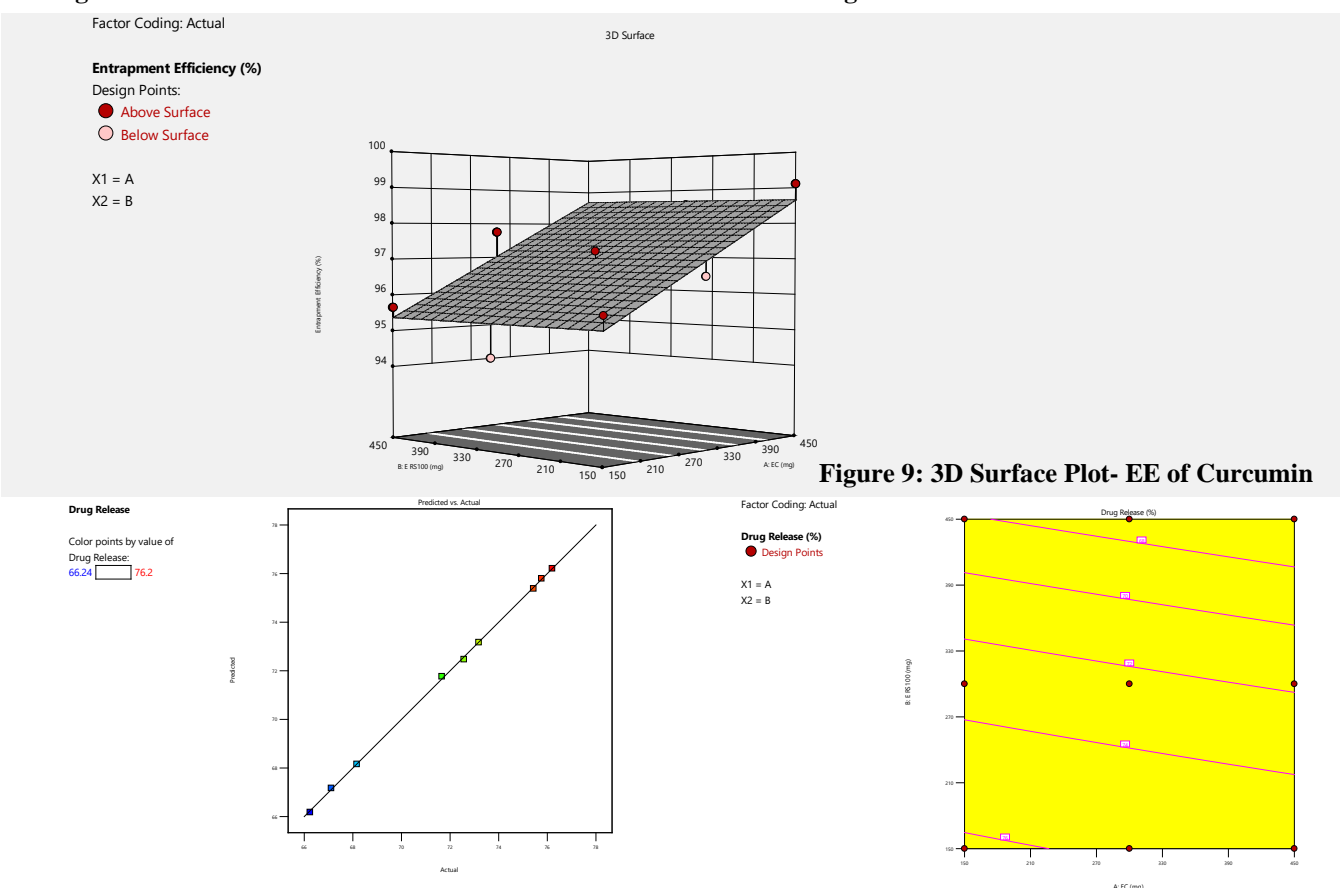
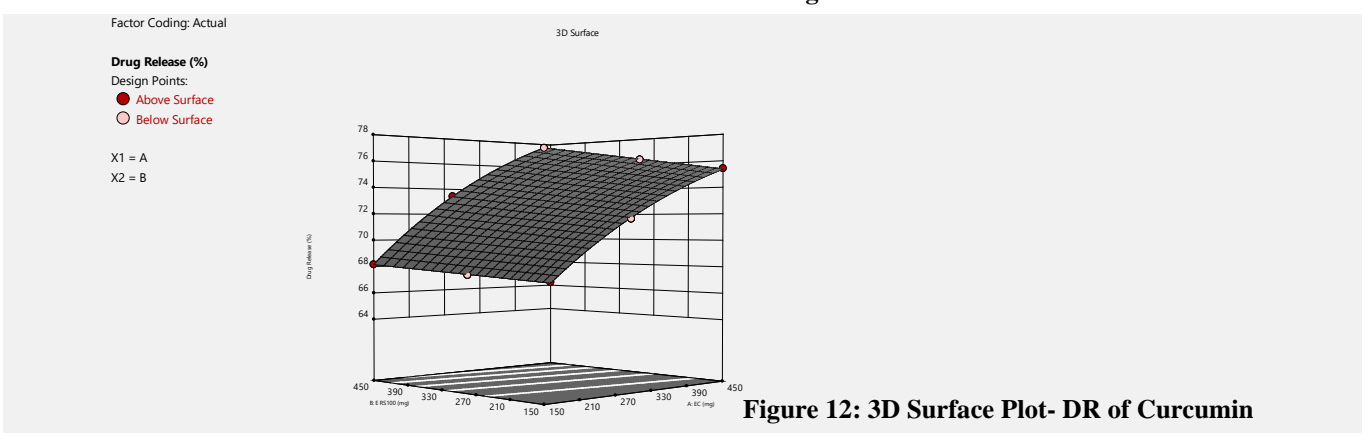


Figure 10: Actual VS Predicted Plot- DR of Curcumin

Figure 11: Contour Plot- DR of Curcumin



#### Response 2: Drug Release

The Actual vs Predicted graph (Figure 10) for the drug release of Curcumin exhibited an R² value of 0.9997, indicating that the QBD outcomes are both significant & exhibit a strong linear relationship. The contour plot (Figure 11) demonstrates that drug release increases as the concentration of Eudragit RS 100 decreases. Consequently, a higher concentration of Ethyl cellulose is recommended to achieve enhanced drug release. Similarly, the 3D surface plot (Figure 12) confirms that lower levels of Eudragit RS 100 correspond with increased Curcumin release, further supporting the suggestion to increase Ethyl cellulose concentration to maximize drug release from the microspheres.

# ANOVA spectra for silymarin from Design Expert software Response 1: Entrapment Efficiency

The Actual vs Predicted graph (Figure 13) shows a very close correlation between the two, with the difference being less than

0.2. The model's Predicted R<sup>2</sup> value of 0.9990 and Adjusted R<sup>2</sup> of 0.9995 indicate a strong agreement, demonstrating the model's reliability.

To validate empirical models, confirmation runs are essential. Entrapment Efficiency exceeds 90%, indicating that both excipients significantly influence this parameter. Increasing the amount of Eudragit RS 100 results in a slight decline in the entrapment efficiency of Silymarin. Conversely, the contour plot (Figure 14) reveals that higher concentrations of ethyl cellulose enhance the microspheres' entrapment efficiency. This trend is further illustrated in the 3D surface plot (Figure 15), where an increase in ethyl cellulose concentration correlates with improved entrapment of Silymarin. At the same time, rising levels of Eudragit RS 100 correspond to a minor decrease in entrapment efficiency.

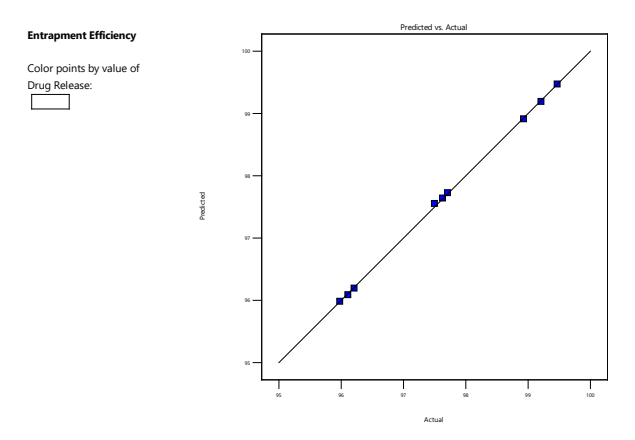


Figure 13: Actual VS Predicted Plot- EE of Silymarin

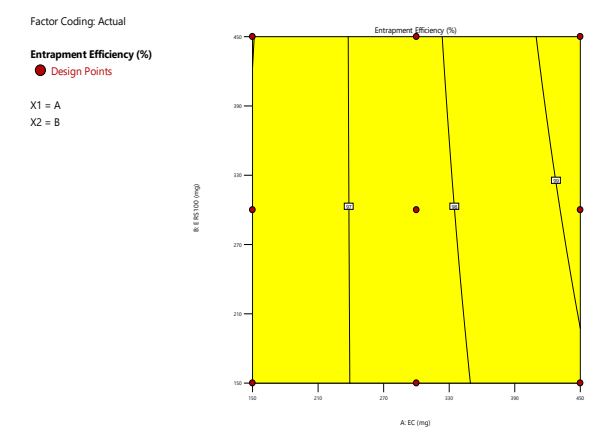
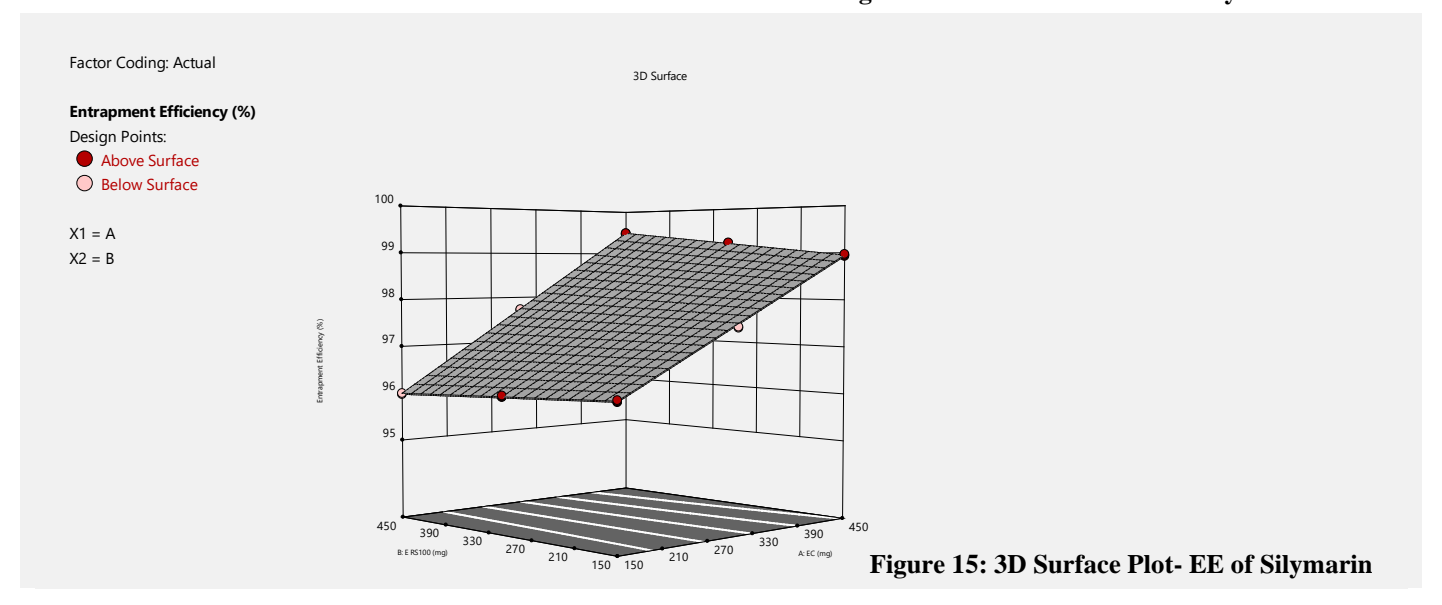


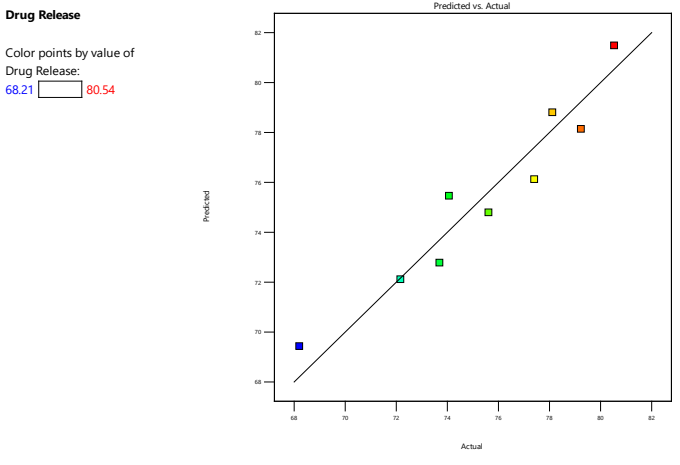
Figure 14: Contour Plot- EE of Silymarin



#### **Response 2: Drug Release**

The Actual vs Predicted graph (Figure 16) for Silymarin drug release demonstrated a coefficient of determination (R2) of 0.9231, indicating that the results from the Quality by Design (QBD) approach are both significant and exhibit a linear relationship. Observing the contour plot (Figure 17), it is evident that reducing the amount of Eudragit RS 100 leads to an increase

in drug release. Therefore, to enhance drug release, a higher conc. of Ethyl cellulose is recommended. Additionally, the 3D surface plot (Figure 18) illustrates that drug release tends to increase when the concentration of Eudragit RS 100 is somewhat lower, while an increase in Ethyl cellulose concentration correlates with greater release of the microspheres.



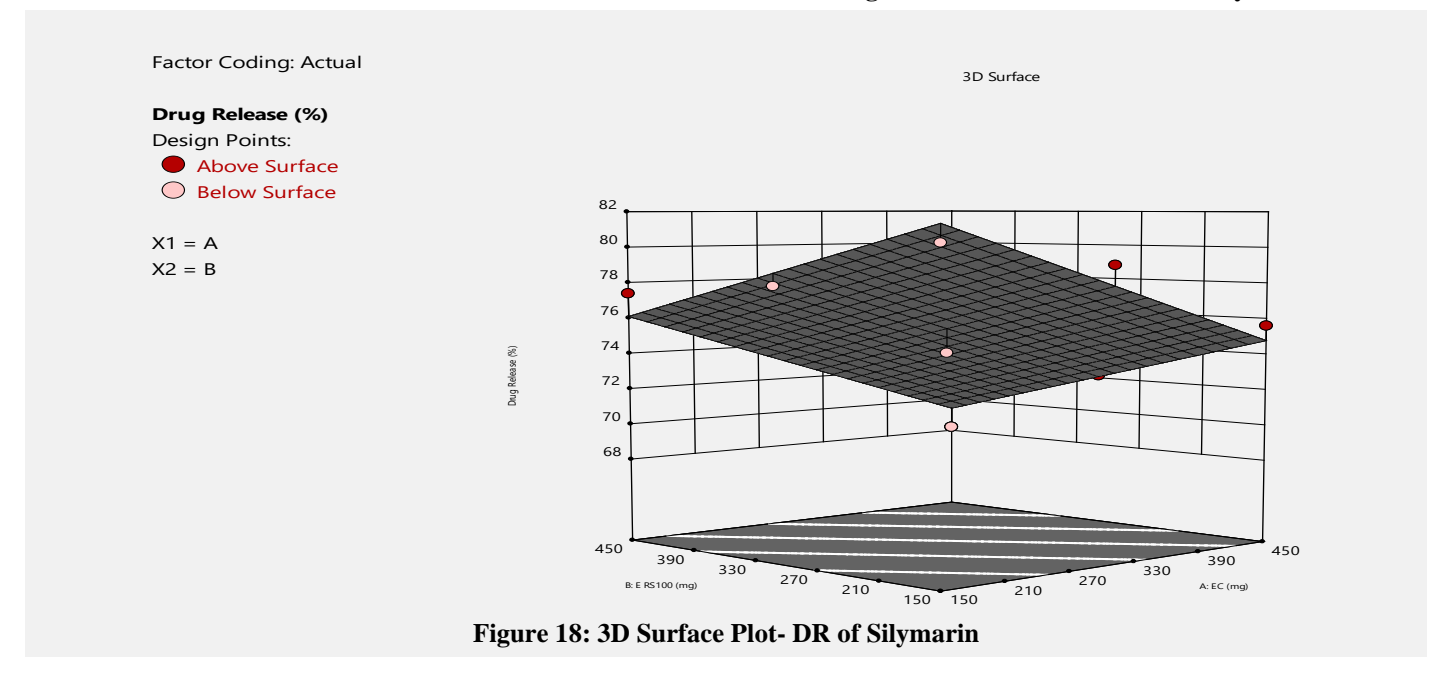
Factor Coding: Actual

Drug Release (%) Design Point

X2 = B

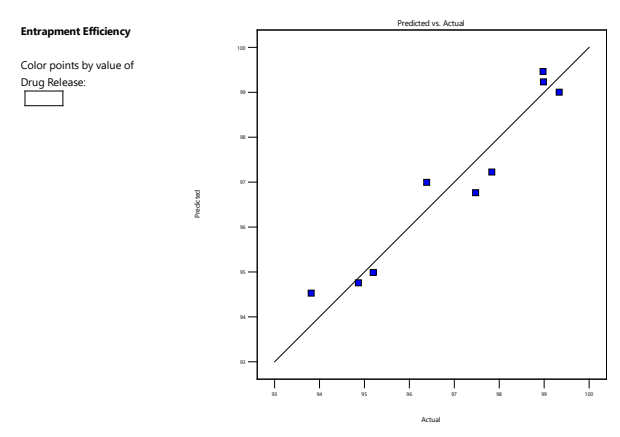
Figure 16: Actual VS Predicted Plot- DR of Silymarin

Figure 17: Contour Plot- DR of Silymarin



#### ANOVA spectrums for piperine from design expert software **Response 1: Entrapment Efficiency**

The Predicted R<sup>2</sup> value of 0.8405 closely matches the Adjusted R<sup>2</sup> value of 0.9091, with a difference under 0.2, indicating good model reliability (Figure 19). Entrapment Efficiency exceeds 90%, suggesting that both excipients significantly influence it. The contour plot (Figure 20) illustrates that increasing Ethyl cellulose concentration while slightly reducing Eudragit RS 100 concentration enhances the entrapment efficiency of the microspheres. Similarly, the 3D surface plot (Figure 21) demonstrates that lower levels of Eudragit RS 100 lead to higher entrapment efficiency of Piperine, and increasing Ethyl cellulose conc. further boosts the microspheres' entrapment efficiency.

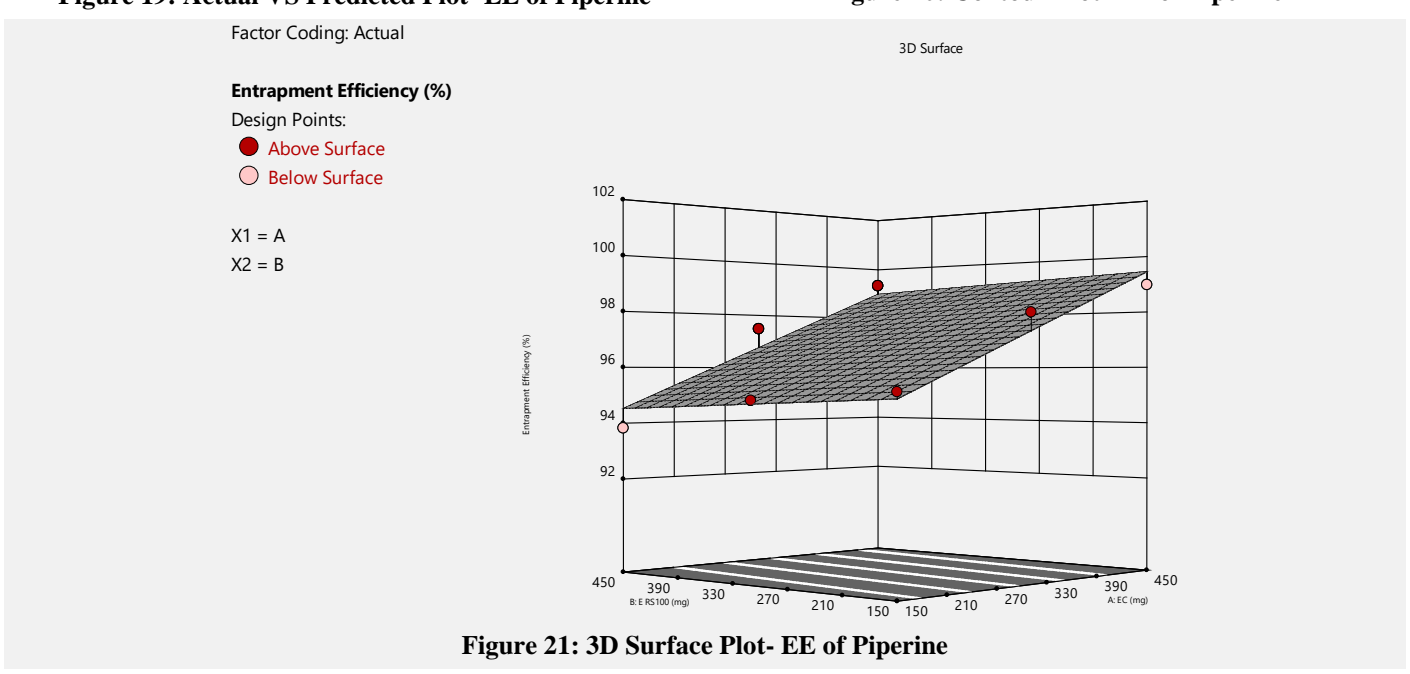


Entrapment Efficiency

Color points by value of Drug Release:

Figure 19: Actual VS Predicted Plot- EE of Piperine

Figure 20: Contour Plot- EE of Piperine



#### **Response 2: Drug Release**

Actual vs Predicted graph (Figure 22) values for Drug release of Piperine showed a R<sup>2</sup> value of 0.9961, implying the QBD results to be significant and linear. It can be observed from the contour

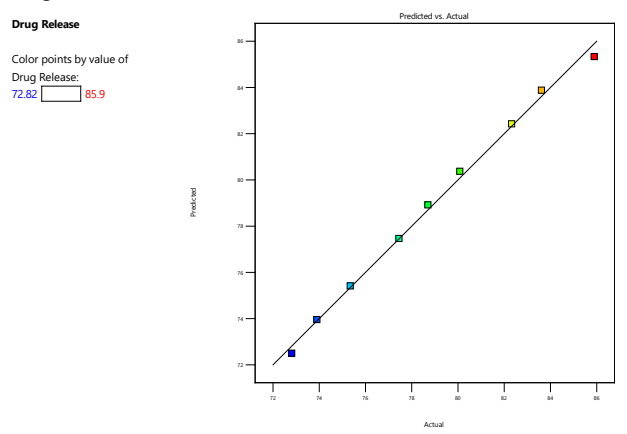


Figure 22: Actual VS Predicted Plot- DR of Piperine

plot (Figure 23) that, with an increase in ethyl cellulose concentration and a decrease in Eudragit RS 100 concentration, the drug release increases. Therefore, it will be advised to concentrate Ethyl cellulose for increased drug release.

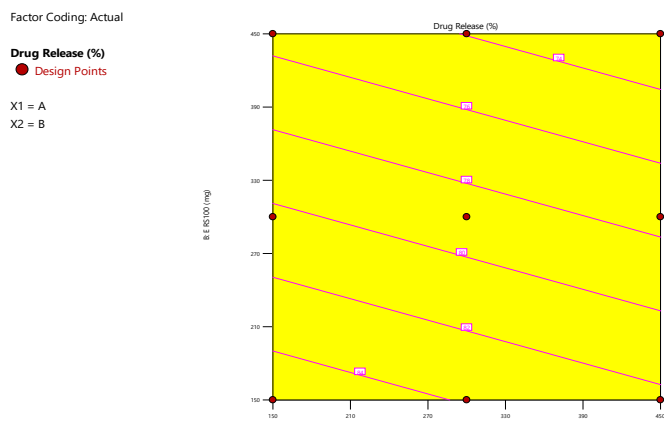
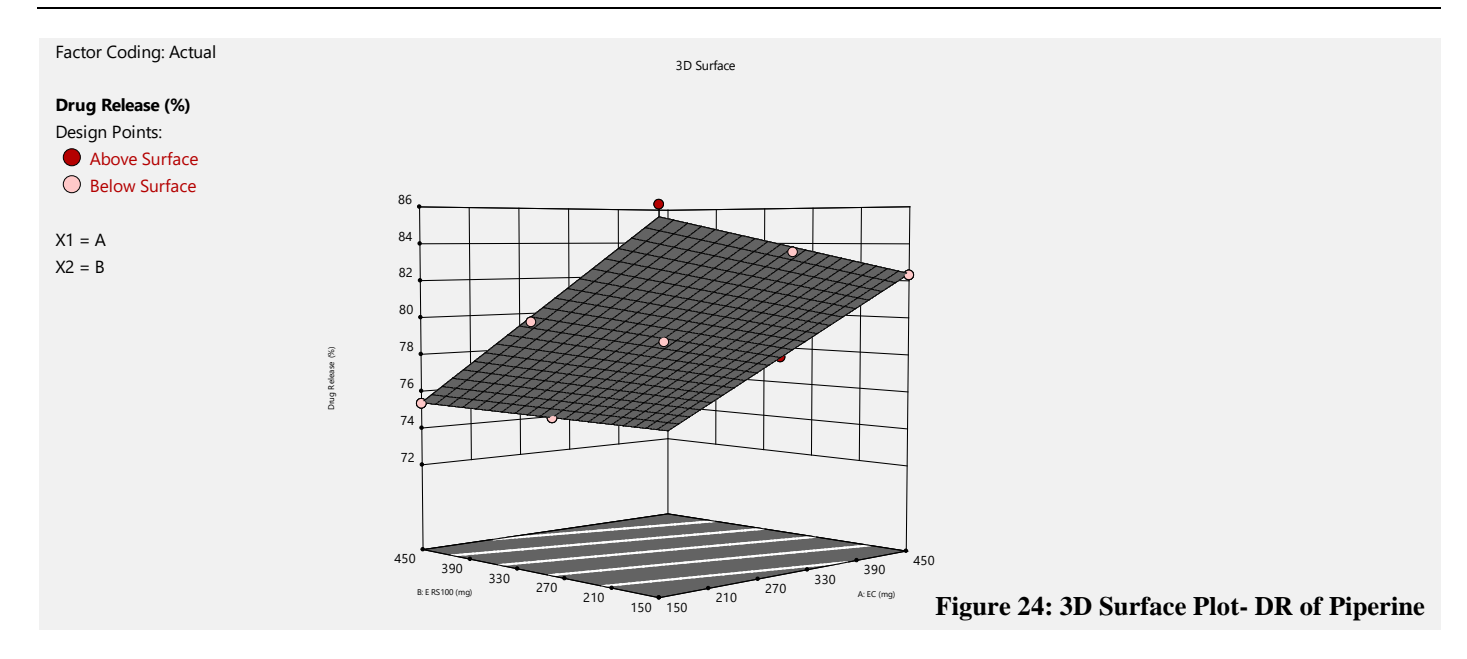


Figure 23: Contour Plot- DR of Piperine



From the 3D surface Plot (Figure 24), it can be seen that piperine release increases when the concentration of Eudragit RS 100 decreases; conversely, the drug release of microspheres increases with an increasing concentration of ethyl cellulose.

#### **CONCLUSION**

The present study successfully developed and optimized gastroretentive floating microspheres containing Silymarin, Curcumin, and Piperine using the solvent evaporation method. Ethyl cellulose and Eudragit RS 100 were identified as effective polymers for achieving high entrapment efficiency, desirable buoyancy, and sustained drug release. The optimized microspheres (F3) exhibited >98% entrapment, 95.94% buoyancy over 8 hours, and sustained drug release (66–73%) fitting zero-order kinetics. These results support their potential in enhancing the oral bioavailability of poorly soluble phytoconstituents for hepatoprotection. However, in vivo evaluation and pharmacokinetic studies are required to confirm clinical relevance. SEM analysis confirmed a spherical morphology with uniform particle size, and stability studies demonstrated the integrity of the formulation over 90 days. These results collectively suggest that the developed microspheres are a promising gastroretentive system for enhancing the therapeutic efficacy and bioavailability of natural hepatoprotective agents. The controlled release profile ensures prolonged gastric residence time, potentially improving clinical outcomes in hepatoprotection. This platform offers a viable strategy for oral delivery of phytoconstituents with limited solubility and rapid gastrointestinal clearance.

#### FINANCIAL ASSISTANCE Nil

#### CONFLICT OF INTEREST

The authors declare no conflict of interest.

#### **AUTHOR CONTRIBUTION**

Misbah Sultana Abdul Kausar Badewale and Varsha Siddheswar Tegeli collected data and performed experiments. Varsha Siddheswar Tegeli conducted the analysis. Misbah Sultana Abdul Kausar Badewale wrote the first draft of the manuscript, and all authors reviewed and revised previous versions. All authors contributed to the study's conception and design and gave final approval.

#### **ABBREVIATIONS**

GRDDS: Gastro-Retentive Drug Delivery System; FDDS: Floating Drug Delivery System; GIT: Gastrointestinal Tract; HCl: Hydrochloric Acid; HPLC: High-Performance Liquid Chromatography; SEM: Scanning Electron Microscopy; EE: Entrapment Efficiency; FTIR: Fourier Transform Infrared Spectroscopy; DSC: Differential Scanning Calorimetry; QbD: Quality by Design; RH: Relative Humidity; ANOVA: Analysis of Variance; DCM: Dichloromethane; µm: Micrometer

#### REFERENCES

[1] Lokhande S. Recent trends in development of gastro-retentive floating drug delivery system: A review. *Asian J. Res. Pharm. Sci.*, **9(2)**, 91–96 (2019) <a href="https://doi.org/10.5958/2231-5659.2019.00014.6">https://doi.org/10.5958/2231-5659.2019.00014.6</a>.

- [2] Sinha S, Thapa S, Singh S, Dutt R, Verma R, Pandey P, Mittal V, Rahman MH, Kaushik D. Development of biocompatible nanoparticles of tizanidine hydrochloride in orodispersible films: in vitro characterization, ex vivo permeation, and cytotoxic study on carcinoma cells. *Current Drug Delivery.*, 19(10), 1061-72 (2022) https://doi.org/10.2174/1567201819666220321111338.
- [3] Luo Q, Ding J, Zhu L, Chen F, Xu L. Hepatoprotective effect of wedelolactone against concanavalin A-induced liver injury in mice. Am. J. Chin. Med., 46(4), 819–833 (2018) <a href="https://doi.org/10.1142/S0192415X1850043X">https://doi.org/10.1142/S0192415X1850043X</a>.
- [4] Kothawade SN, Chaudhari PD. Development of biodegradable porous starch foam for improving oral delivery of eprosartan mesylate. *J of Adv Sci Research.*, **12(03 Suppl 1)**, 120-6 (2021) https://doi.org/10.55218/JASR.s1202112314.
- [5] Masood M, Arshad M, Rahmatullah Q et al. Picrorhiza kurroa: An ethnopharmacologically important plant species of Himalayan region. *Pure Appl. Biol.*, 4, 407–417 (2021) <a href="http://dx.doi.org/10.19045/bspab.2015.43017">http://dx.doi.org/10.19045/bspab.2015.43017</a>.
- [6] Kothawade SN, Avhad SR, Rngade RB, Kotkar RS, Sabale SS, Baviskar AK, Gawade MM. Aloe vera powder as a potent bioenhancer: a comprehensive review. *Int J Pharm Phytopharmacol Res.*, 13(2), 37-44 (2023) https://doi.org/10.51847/ZFFtdBFaPt.
- [7] Kalepu S, Nekkanti V. Insoluble drug delivery strategies: review of recent advances and business prospects. *Acta Pharmaceutica Sinica B.*, 5(5), 442-53 (2015) <a href="https://doi.org/10.1016/j.apsb.2015.07.003">https://doi.org/10.1016/j.apsb.2015.07.003</a>.
- [8] Bhalani DV, Nutan B, Kumar A, Singh Chandel AK. Bioavailability enhancement techniques for poorly aqueous soluble drugs and therapeutics. *Biomedicines.*, 23, 10(9), 2055 (2022) https://doi.org/10.3390/biomedicines10092055.
- [9] Arane PM, Ghanwat DA, Boyane V, Kothawade SN, Doshi P. Preparation and in Vitro Characterization of Eprosartan Mesylate Solid Dispersions using Skimmed Milk Powder as Carrier. *Int J of Adv in Pharm Res.*, 2(12), 658-65 (2011) <a href="https://doi.org/10.5530/ijper.50.3.31">https://doi.org/10.5530/ijper.50.3.31</a>.
- [10] Gupta R, Chen Y, Xie H. In vitro dissolution considerations associated with nano drug delivery systems. Wiley Interdisciplinary Reviews: *Nanomedicine and Nanobiotechnology.*, 13(6), e1732 (2021) <a href="https://doi.org/10.1002/wnan.1732">https://doi.org/10.1002/wnan.1732</a>.
- [11] Shabbir M, Sajid A, Hamid I, Sharif A, Akhtar MF, Raza M, Ahmed S, Peerzada S, Amin MU. Influence of different formulation variables on the performance of transdermal drug delivery system containing tizanidine hydrochloride: in vitro and ex vivo evaluations. *Braz J of Pharma Sci.*, **54**, e00130 (2019) https://doi.org/10.1590/s2175-97902018000400130.
- [12] Kaurav H, Tripathi M, Kaur SD, Bansal A, Kapoor DN, Sheth S. Emerging trends in bilosomes as therapeutic drug delivery

- systems. *Pharmaceutics.*, **16(6)**, 697 (2024) https://doi.org/10.3390/pharmaceutics16060697.
- [13] Pınar SG, Oktay AN, Karaküçük AE, Çelebi N. Formulation strategies of nanosuspensions for various administration routes. *Pharmaceutics.*, **15**(**5**), 1520 (2023) https://doi.org/10.3390/pharmaceutics15051520.
- [14] He S, Mu H. Microenvironmental pH modification in buccal/sublingual dosage forms for systemic drug delivery. *Pharmaceutics.*, **15(2)**, 637 (2023) <a href="https://doi.org/10.3390/pharmaceutics15020637">https://doi.org/10.3390/pharmaceutics15020637</a>.
- [15] Kallakunta VR, Sarabu S, Bandari S, Tiwari R, Patil H, Repka MA. An update on the contribution of hot-melt extrusion technology to novel drug delivery in the twenty-first century: Part I. Expert Opin Drug Deliv., 16(5), 539-50 (2019) https://doi.org/10.1080/17425247.2019.1609448.
- [16] Kapoor DU, Vaishnav DJ, Garg R, et al. Exploring the impact of material selection on the efficacy of hot-melt extrusion. *Int J Pharm.*, 668, 124966 (2025) <a href="https://doi.org/10.1016/j.ijpharm.2024.124966.">https://doi.org/10.1016/j.ijpharm.2024.124966.</a>
- [17] Dinesh Kumar. Various Aspects of Solid Dispersion Technology: A Review. Res J Pharm Technol., 18(4), 1872-8 (2025) <a href="https://doi.org/10.52711/0974-360X.2025.00267">https://doi.org/10.52711/0974-360X.2025.00267</a>.
- [18] Kaurav H, Tripathi M, Kaur SD, Bansal A, Kapoor DN, Sheth S. Emerging trends in bilosomes as therapeutic drug delivery systems. *Pharmaceutics.*, 16(6), 697 (2024) https://doi.org/10.3390/pharmaceutics16060697.
- [19] Rampurawala M, Shah C, Upadhyay U. Nano-Suspension: A Novel and Emerging Approach in Pharmaceutical Drug Delivery. *Int. J. of Pharm. Sci.*, 2(9), 133-46 (2024) <a href="https://doi.org/10.5281/zenodo.13629942">https://doi.org/10.5281/zenodo.13629942</a>.
- [20] Mura P, Fenyvesi F. Development of Oral Tablets of Nebivolol with Improved Dissolution via Cyclodextrin Complexation. *Molecules.*, 29(10), 1234 (2024) https://doi.org/10.3390/molecules290101234.
- [21] Smruti PC, Gupte A. Solid Dispersions Obtained by Ball Milling as Delivery Platform for ETD—Improved Solubility and Dissolution. *Materials.*, 17(16), 3923 (2022) <a href="https://doi.org/10.3390/ma17163923">https://doi.org/10.3390/ma17163923</a>.
- [22] PDA Technical Report Authors. Hot-Melt Extrusion: An Emerging Technique for Solubility Enhancement of Poorly Water-Soluble Drugs. PDA J Pharm Sci Technol., 75(4), 357-65 (2021) https://doi.org/10.5731/pdajpst.2019.011403.
- [23] Joshi K, Chandra A, Jain K, Talegaonkar S. Nanocrystalization: an emerging technology to enhance the bioavailability of poorly soluble drugs. *Pharmaceu Nanotech.*, 7(4), 259-78 (2019) <a href="https://doi.org/10.2174/2211738507666190405182524">https://doi.org/10.2174/2211738507666190405182524</a>.